

Conjugated Poly(phenylacetylene) Films Cross-Linked with Electropolymerized Polycarbazole Precursors

Timothy Fulghum,[†] S. M. Abdul Karim,[‡] Akira Baba,[†] Prasad Taranekar,[†] Takafumi Nakai,[‡] Toshio Masuda,^{*,‡} and Rigoberto C. Advincula^{*,†}

Department of Chemistry, University of Houston, Houston, Texas 77204-5003, and Department of Polymer Chemistry, Graduate School of Engineering, Kyoto University, Kyoto 606-8501, Japan

Received May 27, 2005; Revised Manuscript Received November 27, 2005

ABSTRACT: In this work, we describe the synthesis and electropolymerization of conjugated substituted polyacetylenes, poly(*N*-alkoxy-(*p*-ethynylphenyl)carbazole) or **PPA-Cz-Cn** with electropolymerizable carbazole side groups to form conjugated polymer network (CPN) films. The phenylacetylene monomer was functionalized with a carbazole group separated by an alkylene spacer. Polymerization of the monomer in solution is accomplished using a Rh catalyst to form a “precursor polymer”. The electrochemical behavior and cross-linking of the carbazole side group was then investigated by cyclic voltammetry (CV) and spectroelectrochemistry. A trend in the redox electrochemical behavior was observed with varying alkyl spacer length between the poly(phenylacetylene) backbone and carbazole side-group. The resulting film combines the electrooptical properties of the conjugated poly(phenylacetylene) polymer with polycarbazole units in a cross-linked electropolymerized film as evidenced by the CV and spectroelectrochemical behavior. This study emphasizes the preparation of polymer materials with mixed π -conjugated species arising from the electrochemical cross-linking of a designed precursor polymer.

Introduction

Polyacetylene is one of the first reported conductive polymers with both high conductivity and interesting electrooptical properties.¹ They have been synthesized using a variety of catalysts and polymerization conditions, often under inert atmosphere. Substituted polyacetylenes derivatives have also been extensively studied and are readily synthesized by a variety of metal carbene and metal halide catalysts.² A key advantage of substituted polyacetylenes is their stability and solubility compared to polyacetylenes at ambient conditions. Using metathesis polymerization techniques with group V and VI metal catalysts, their configuration and conformation (*cis*–*trans* and *cisoidal*–*transoidal*) can be controlled toward higher or lower π -conjugation lengths. On the other hand, Rh catalysts are known to control the formation of *cis* and *trans* configurations on the polymer backbone primarily through an insertion mechanism.³ The polymerization of poly(phenylacetylene)s (PPA) is well-known and has been thoroughly investigated.⁴ While substituted polyacetylenes have been investigated for various electrooptical and nonlinear optical applications,⁵ they have been less studied as materials for electroluminescent devices and organic semiconductors. However, several reports by our group and others have shown electroluminescence properties based on fluorophore incorporation and active charge-carrier transport property optimization for these type of polymers.⁶

Poly(*N*-vinylcarbazole) (PVK) materials have been extensively studied.⁷ They exhibit interesting electrical and optical properties as light emitting diode materials,^{8,9} solar cells,¹⁰ and applications in various electrochromic devices.^{11,12} Specifically, PVK shows good hole-transport properties which have important applications for improving the performance of organic electroluminescent devices.¹³ Others have reported applications in amperometric chemical sensors.¹⁴ PVK exhibits these interesting

properties primarily due to the carbazole group. On the other hand, an *all* 3,6-position linkage of the carbazole units will lead to the formation of conjugated poly(3,6-*N*-vinylcarbazole).^{15,16} The synthesis of polycarbazoles (PCz) is also of great interest for electrical conductivity and electrochromic device applications. Several groups have investigated its electropolymerization on Pt and Au substrates.¹⁷

Recently, several groups including our group have reported the conversion of “precursor polymers” to form conjugated polymer network (CPN) films on conducting surfaces.¹⁸ The approach consists of synthesizing a precursor polymer, which by design contains pendant electroactive monomer units. Electropolymerization or chemical oxidation results in a conjugated polymer network having both *inter*- and *intramolecular* cross-linkages between the pendant monomer units. The films formed are characterized by high optical quality (transparency), uniform coverage, good adhesion, smoothness in morphology, and controlled ion permeability.¹⁹ Moreover, by controlling the amount of conjugated species and doping, it should be possible to control electrical conductivity.^{20,29a} Thus, the process is interesting for depositing *insoluble* cross-linked ultrathin films of conjugated polymers for practical electrooptical applications. A variety of combinations should be possible for the design of a precursor polymer backbone and the “electroactive monomer” side group to form the CPN film. It is also possible to *copolymerize* with small molecule electroactive monomers with varying compositions in order to control the degree of cross-linking and linear polymer formation. We have applied these materials to a number of possible applications toward electroluminescent devices.²¹ We have also previously reported the surface grafting of carbazole-functionalized polyfluorenes on carbazole self-assembled monolayer (SAM) modified indium tin oxide (ITO) surfaces.²²

With the interest in combining the electrooptical properties of PPA and PCz in a CPN film, we have synthesized a series of substituted poly(phenylacetylene)s containing carbazole unit side groups. As previously mentioned, the stereochemical

[†] University of Houston.

[‡] Kyoto University.

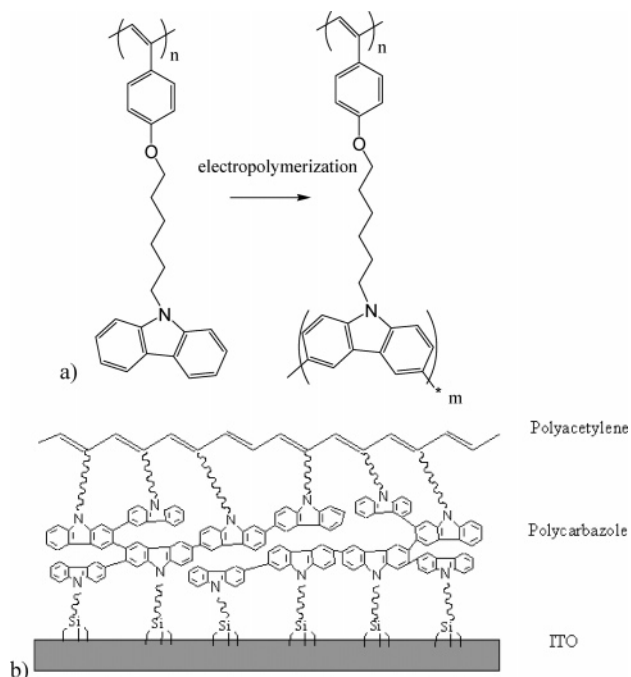
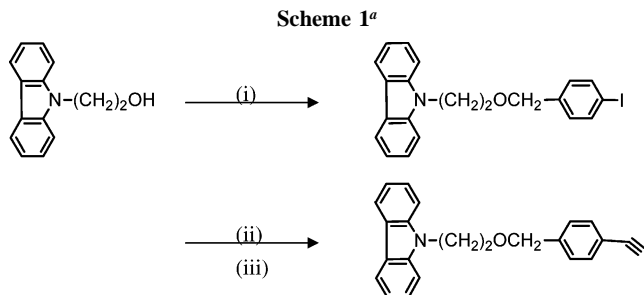


Figure 1. Electropolymerization and cross-linking scheme for carbazole substituted polyacetylene: (a) the chemical structure of the precursor polymer and a cross-linked unit; (b) electrografting of the polymer to a SAM-modified ITO electrode surface.

microstructure of poly(phenylacetylene) can be controlled using metal catalysts. Rh catalysts can preferentially give cis-rich polymers while W catalysts give trans-rich polymers. We have previously reported the synthesis, characterization, and electroluminescence properties of soluble poly(phenylacetylene)s with pendant carbazole groups.²³ The effective conjugation length of the PPA backbone played an important role in photoluminescence (PL) quantum efficiency and photoconductivity. However, detailed electrochemical cross-linking studies have not been reported toward CPN film formation and their possible application to devices. This work details the formation of CPN films using this type of PPA precursor materials where the carbazole moiety is separated by an alkyl spacer (Figure 1a). With a PPA polymer backbone, the carbazole side groups can then be used for secondary polymerization (cross-linking) through the carbazole units. In this case, it is important to facilitate the electropolymerization *without decomposing* the PPA main chain. The precursor polymer was polymerized on bare ITO and Au films, as well as, a self-assembled monolayer (SAM) carbazole modified "electroactive" ITO surface to probe differences in film formation.²² The polymer can be electrografted to the substrate resulting in robust insoluble films combining the properties of PPA and PCz (Figure 1b). The polymerization mechanism was investigated in situ using UV-vis spectroelectrochemistry and multiple cyclic voltammetry (CV) techniques, the morphology were examined with atomic force microscopy (AFM).

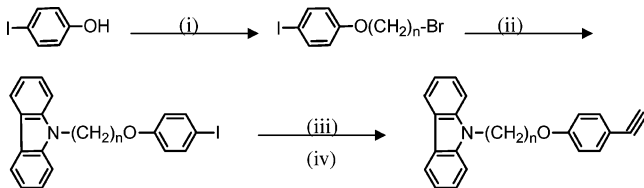
Experimental Section

Materials. All the reagents for monomer synthesis were commercially available and used without further purification. The toluene solvent used in the polymerization was distilled and purified over CaH₂. The Rh catalyst, [(nbd)RhCl]₂, was purchased from Aldrich and used as received. For the electrochemical studies, tetrabutylammonium hexafluorophosphate (TBAH), also from Aldrich) was dried in vacuo at 40 °C for a day. Predistilled THF was dried by refluxing over a benzophenone-sodium complex for a half day.



^a (i) *p*-Iodobenzyl bromide, NaH, THF, 0 °C, 12 h. (ii) trimethylsilylacetylene, PdCl₂(PPh₃)₂, PPh₃, CuI, Et₃N, 25 °C, overnight. (iii) MeOH/C₆H₆, NaOH_{aq}, 60 °C, 3 h.

Scheme 2. Synthetic Scheme of Cz-C6 and Cz-C8^a



^a (i) Br(CH₂)_nBr, K₂CO₃, acetone, reflux, 5 h. (ii) Carbazole, C₆H₆, NaOH_{aq}, tetrabutylammonium bromide, reflux. (iii) Trimethylsilylacetylene, PdCl₂(PPh₃)₂, PPh₃, CuI, Et₃N, 25 °C, overnight. (iv) MeOH/C₆H₆, NaOH_{aq}, 60 °C, 3 h.

Monomer Synthesis for PPA-Cz-Cn series. Carbazole substituted phenylacetylene monomers with various alkyl chain lengths, e.g., C3, C6, and C8 (abbreviated as **Cz-C3**, **Cz-C6** and **Cz-C8**, respectively) were synthesized.²⁴ Monomer **Cz-C3** was synthesized according to Scheme 1. The total yield of **Cz-C3** was 58%. The synthetic route to monomer **Cz-C6** and **Cz-C8** is shown in Scheme 2. The yields of **Cz-C6** and **Cz-C8** were 39% and 49%, respectively. The structure and purity of the monomers were confirmed by NMR, IR, and elemental analysis and is described as follows:

N-Ethyl(*p*-ethynylbenzyloxy)carbazole, Cz-C3. Yellowish crystal. Yield: 58%. Mp: 94.0 °C. ¹H NMR (400 MHz, CDCl₃): δ (ppm) 3.04 (s, 1H), 3.85 (t, 2H, *J* = 5.6 Hz), 4.37 (s, 2H), 4.51 (t, 2H, *J* = 5.6 Hz), 7.05 (d, 2H, *J* = 8.8 Hz), 7.20–7.45 (m, 8H), 8.09 (d, 2H, *J* = 8.0 Hz). IR (KBr, cm⁻¹): 3274, 2888, 2865, 1626, 1597, 1485, 1462, 1453, 1327, 1154, 1021, 745, 725. Anal. Calcd For C₂₃H₁₉NO: C, 84.89; H, 5.89; N, 4.30; O, 4.92. Found: C, 84.68; H, 5.85; N, 4.11; O, 4.85.

N-Hexoxy(*p*-ethynylphenyl)carbazole, Cz-C6. White crystal. Yield: 39%. Mp: 81.6 °C. ¹H NMR (400 MHz, CDCl₃): δ (ppm) 1.40–1.55 (m, 4H), 1.74 (m, 2H), 1.93 (m, 2H), 3.02 (s, 1H), 3.89 (t, 2H, *J* = 6.0 Hz), 4.34 (t, 2H, *J* = 6.8 Hz), 6.77 (d, 2H, *J* = 8.8 Hz), 7.20–7.48 (m, 8H), 8.10 (d, 2H, *J* = 8.0 Hz). IR (KBr, cm⁻¹): 3256, 3052, 2940, 1607, 1509, 1483, 1462, 1453, 1327, 1154, 1021, 750, 725. Anal. Calcd For C₂₆H₂₅NO: C, 84.98; H, 6.86; N, 3.81; O, 4.35. Found: C, 84.76; H, 6.83; N, 3.57; O, 4.13.

N-Octoxy(*p*-ethynylphenyl)carbazole, Cz-C8. White crystal. Yield: 49%. Mp: 80–81 °C. ¹H NMR (400 MHz, CDCl₃): δ (ppm) 1.10–1.50 (m, 8H), 1.73 (m, 2H), 1.86 (m, 2H), 2.98 (s, 1H), 3.89 (t, 2H, *J* = 6.4 Hz), 4.28 (t, 2H, *J* = 6.8 Hz), 6.78 (d, 2H, *J* = 8.8 Hz), 7.20–7.48 (m, 8H, *J* = 8.0 Hz), 8.09 (d, 2H). IR (KBr, cm⁻¹): 3256, 2855, 1607, 1509, 1483, 1462, 1451, 1325, 1156, 1015, 750, 727. Anal. Calcd For C₂₈H₂₉NO: C, 85.02; H, 7.39; N, 3.54; O, 4.04. Found: C, 84.80; H, 7.43; N, 3.27; O, 4.15.

Polymerization To Form PPA-Cz-Cn. Poly(phenylacetylene)s were prepared by metal-catalyzed polymerization using a Rh catalyst according to the literature.²⁵ Polymerizations were performed in a Schlenk tube equipped with a three-way stopcock under nitrogen atmosphere. Unless otherwise specified, the polymerization conditions were as follows: In toluene, 30 °C, 24 h; [M]₀ = 200 mM, [Cat] = 1.0 mM, and [Cocat] = 2 mM. Polymers were isolated by precipitation in a large excess of methanol, separated by filtration, and the yields of the polymers determined by

gravimetry. A control poly(phenylacetylene) (PPA) sample was also polymerized for comparison purposes.

Synthesis of Triethoxy(11-carbazoylundecyl)silane SAM. The synthesis of triethoxy(11-carbazoylundecyl)silane was carried out as previously reported.²³ The 9-undec-10-enyl-9H-carbazole was synthesized by the reaction between carbazole and 11-bromoundec-1-ene with potassium hydroxide in 20 mL DMF at room temperature. 9-Undec-10-enyl-9H-carbazole, triethoxysilane, and H_2PtCl_6 were charged in a one-neck flask under nitrogen. The flask was sealed and put into a sonicating bath to yield the triethoxy(11-carbazoylundecyl)silane.²⁶

SAM Modification of the ITO. The triethoxy(11-carbazoylundecyl)silane (Figure 1) was used to modify all the ITO surfaces by SAM. ITO was cleaned using standard sonicating solutions (2% glass cleaning solution) followed by copious water rinsing and last by argon ion plasma treatment. The ITO was treated by the 1% triethoxy(11-carbazoylundecyl)silane solution in toluene at 60 °C for 3 days. The slides were then rinsed successively with toluene and THF then dried by a dry nitrogen flow.

Instrumentation and Electropolymerization Setup. The molecular weights of the polymers were determined by gel permeation chromatography (GPC) on a Jasco Gulliver system (PU-980, CO-965, RI-930, and UV-1570). Elution was done on Shodex columns K804, K805, and J806 with CHCl_3 as eluent at a flow rate of 1.0 mL/min and calibrated with polystyrene (PSt) standards. FT-IR spectra, UV-vis spectra, and NMR spectra were recorded on a Shimadzu FT-IR-8100 spectrophotometer, a Jasco V-550 spectrophotometer, and a JEOL Ex-400 spectrometer, respectively. Thermogravimetric analysis (TGA) was conducted in air on a Perkin-Elmer TGA7 thermal analyzer.

The cyclic voltammetry (CV) experiments were carried out on a Princeton Applied Research Parstat 2263 with a modified ITO substrate as the working electrode coupled with a Pt plate counter and Ag/AgCl reference electrode. Cyclic voltammetry was utilized to prepare the cross-linked films from a 0.1 wt % of the precursor polymer solution of 0.1 M TBAH/ CH_2Cl_2 , where TBAH = tetrabutylammonium hexafluorophosphate. Copious washing with CH_2Cl_2 solvent and dry nitrogen drying was done prior to any film analysis.

Electrochemical-quartz crystal microbalance (QCM) measurements were performed on a R-QCM (Maxtek Inc.) with an Amel 2049 potentiostat/galvanostat and Power lab system utilizing the QCM crystal as the working electrode and a Pt plate as counter and Ag/AgCl reference electrode. The QCM apparatus, probe, and crystals are also available from Maxtek Inc. The diameter of the polished QCM crystals (5 MHz) is 13 mm. The data acquisition was done with an R-QCM system equipped with an inbuilt phase lock oscillator and the R-QCM Data-Log software. The gold electrodes were cleaned with a plasma etcher (Plasmod, March) prior to use.

Spectroelectrochemical UV-vis measurements of the films were carried out in situ on an ITO substrate. This was done using a Teflon flow cell manufactured with a modified ITO window and microscope slide window that was placed in the path of an HP-8453 diode array spectrometer.

Atomic force microscopy (AFM) imaging was examined in ambient conditions with a PicoSPM II (PicoPlus, Molecular Imaging) in the Magnetic AC mode (MAC mode). MAC mode uses a magnetic field to drive a magnetically coated cantilever in the top-down configuration. Type II MAC levers with a spring constant of 2.8 nN/M with about 10 nm tip radius were used for all scans.

Results and Discussion

Polymerization of Phenylacetylenes. The carbazole functionalized phenylacetylene monomers were characterized by FT-IR, NMR, and elemental analysis. The polymerization conditions and results for poly(*N*-ethyl(*p*-ethynylbenzyloxy)carbazole), **PPA-Cz-C3**, poly(*N*-hexoxy(*p*-ethynylphenyl)carbazole), **PPA-Cz-C6**, and *N*-octoxy(*p*-ethynylphenyl)carbazole, **PPA-Cz-C8**

Table 1. Summary of Polymerization of Cz-C3, Cz-C6, and Cz-C8 with $[(\text{nbd})\text{RhCl}_2]^a$

monomer	[M]/[Cat]	yield, %	$M_n/10^3$ ^b	M_w/M_n ^b	solubility ^c
Cz-C3	200	100			insoluble
	60	53	148.0	1.46	partly soluble
Cz-C6	200	100			insoluble
	60	87	109.6	10.95	soluble
Cz-C8	200	100			insoluble
	60	89	93.9	1.74	soluble

^a In toluene, at 30 °C. ^b By GPC (eluent CHCl_3 PSt standard). ^c In THF, CHCl_3 , DMF etc.

are summarized in Table 1. When the concentration of catalyst is low, a $\sim 100\%$ yield can be obtained. However, the ensuing product was insoluble in any solvent and could not be easily characterized.²⁷ Decreasing the monomer-to-catalyst ratio yielded soluble polymers but at lower yield. This latter route was taken in order to obtain soluble polymers suitable for our electropolymerization experiments. **PPA-Cz-C3** was obtained as an orange solid, while **PPA-Cz-C6** and **PPA-Cz-C8** were yellow powders. The polymers obtained at lower monomer-catalyst ratio (60:1) were partly or completely soluble in organic solvents such as CHCl_3 , THF, DMF, etc., but totally insoluble in alkanes or alcohols. According to the GPC results, the number-average molecular weights (M_n) of **PPA-Cz-C3**, **PPA-Cz-C6**, and **PPA-Cz-C8** were 148.0×10^3 , 109.6×10^3 , and 93.9×10^3 , respectively. These molecular weight values are consistent with previously reported PPA derivatives using similar conditions.²³ Characterization of the polymers was also done by IR and NMR. The IR spectra of the polymers exhibited no absorption band around 3300 cm^{-1} , usually attributed to the stretching vibration of $\text{C}\equiv\text{C}$ bond, which was seen in the monomers. In the ^1H NMR spectra of the polymers, a signal at around 3.0 ppm assigned to the acetylenic proton of monomers was not observed. All of these results clearly point to the reaction of the triple bonds of the monomers to form polymer main chains composed of alternating single-double bonds. It is known that Rh catalysts provide poly(phenylacetylenes) with cis-transoidal structures, showing a signal due to the olefinic proton of the main chain around 6 ppm.²³ In fact, with the ^1H NMR spectra of the polymers, a resonance around 5.8 ppm was indeed observed, indicating the cis-transoidal structure of the backbone. From the integrated intensities of the olefinic proton and two carbazoyl protons (ca. 8.1 ppm), the cis contents were determined to be 74%, 64% and 93% for **PPA-Cz-C3**, **PPA-Cz-C6**, and **PPA-Cz-C8**, respectively. According to the TGA trace, the weight loss of the polymers in air occurred above 370 °C, whereas that of poly(phenylacetylene)s usually starts at 250 °C. These results suggest that these polymers have superior thermal stability compared to typical poly(phenylacetylene)s.¹⁻⁴

The normalized UV-vis spectra of the neutral **PPA-Cz-C6** and **PPA** are shown in Figure 2. The absorbance spectra of the **PPA-Cn-Cz** are consistent with the fact that carbazoyl moieties were incorporated as polymer side groups. The absorption band, tailing from 350 to 450 nm with an onset at 500 nm is due to the absorption ($\pi-\pi^*$) of the poly(phenylacetylene) main chain. This onset is similar for both, indicating little conformational change attributed to the addition of the carbazoyl groups. The other peaks below 350 nm were attributed to the absorption by the $\pi-\pi^*$, $n-\pi^*$, and benzenoid transitions of carbazole and phenyl groups. The conjugation length of these polymers is typical of most PPAs. The electrooptical band gap, ΔE_g , of the un-cross-linked polymer can be calculated from the onset of absorbance and is equivalent to 2.46 eV, which is typical of poly(phenylacetylene)s.²⁻⁴

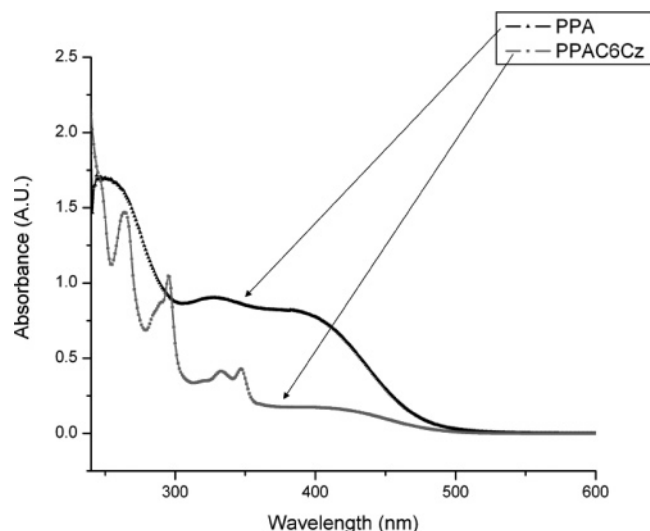


Figure 2. Comparative UV-vis solution spectra of PPA and PPA-C6-Cz polymers.

CV of Poly(phenylacetylene) (PPA). Solution electrochemical studies were first performed on PPA to determine the stability of the polymer to the electrochemical window of choice for precursor polymer electropolymerization. No oxidation was seen on the anodic scan up to a potential of 1.8 V. (Supporting Information). This indicates that there is no degradation in the polymer backbone if the experiments were limited at this potential window.²⁸ Consistently, no film formation was observed on the substrate upon subsequent potential cycling due to the lack of electropolymerizable units and the preserved solubility of the polymer.

We have recently investigated the electrochemical polymerization and cross-linking of poly(vinyl-*N*-carbazole) through the carbazole units.²⁹ This linkage can be formed by oxidation involving a three-electron transfer process with pendant carbazole ring dimerization occurring first via the 3,6-position leading to intermolecular cross-linking. The intermediate is believed to be based on a carbazolium radical cation which rapidly reacts via coupling-deprotonation to form the dimer.¹⁶ Subsequent cycles lead to higher oligomeric species and further cross-linking as evidenced by a lowering of the oxidation potential and increase of charge with each succeeding cycle.

Figure 3a,b shows the CV traces for the polymer **PPA-Cz-C6** showing the CV deposition and the precursor polymer-free scan, respectively. The electrochemical experiment was done in 0.1 M TBAH/CH₂Cl₂ electrolyte at a scan rate of 100 mV s⁻¹. The CV scan for the other polymers are shown in the Supporting Information. In this system, the onset of oxidation of the tethered carbazole monomer was observed to occur at about 0.9 V on the first cycle, forming the first layer of conjugated polycarbazole network film. Subsequent cycles showed the same onset, but including the oxidation peak (doping) of the deposited films which appears at about 0.7–0.8 V range. This is proven by the precursor polymer-free scan of the deposited polymer film showing no increase at 1.0 V but retains the peak at 0.8 V even with six cycles (Figure 3b). The reduction peak in the cathodic scan is observed around 0.6 V. This value is also preserved in the precursor-polymer free CV scan. This means that if the electrochemical potential can be controlled to be lower than 1.1 V it is possible to observe polymerization (cross-linking) through the carbazole units without decomposition of the poly(phenylacetylene) backbone for these polymers.

For the CV deposition of the films, the oxidative doping was generally observed at about 0.7–0.8 V and followed by another

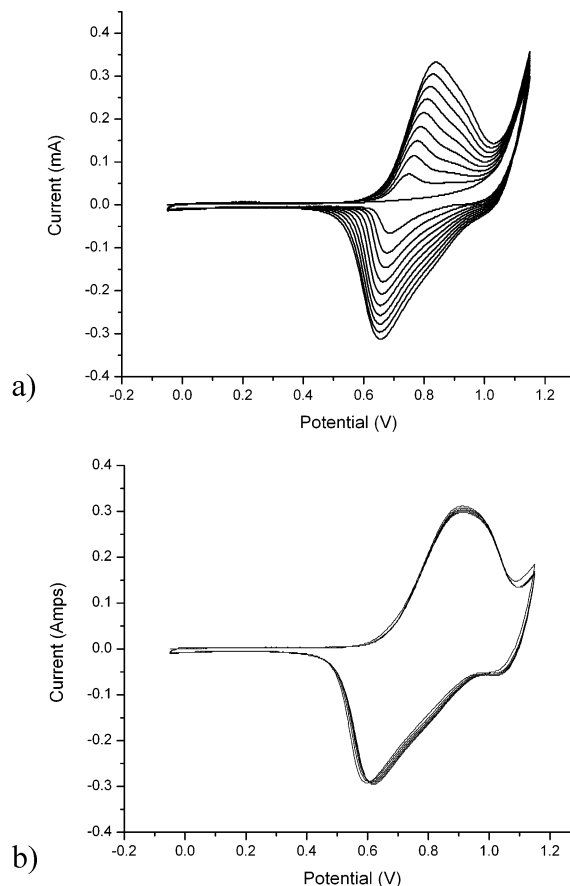


Figure 3. (a) Ten cycle CV for electrochemical cross-linking/deposition of **PPA-C6-Cz** at a scan rate of 100 mV/s. (b) Six cycle CV for electrochemical doping/dedoping of the deposited **PPA-C6-Cz** film at a scan rate of 100 mV/s.

current increase at about 1.0 V during the anodic scan of the cycle. Similar to PVK, the first cycle always showed an oxidation onset at 0.9 V and the appearance of the oxidation-doping peak in the 0.6–0.7 V range with subsequent cycles.^{15–17} This means that the appearance of the 0.7 V peak is indeed due to the presence of the cross-linked carbazole units, regardless of the polymer backbone. All the CVs were reversible in the oxidation-reduction cycles at scan rates within the 20–100 mV/s range. Like other polyacetylenes, these polymers exhibited p-doping behavior.³⁰ Thus, these observations point to a well-controlled electrochemical and cross-linking behavior which should allow work-function tuning when applied to actual LED devices using ITO substrates.^{21a} Recently, extensive electrochemical studies on a class of polyacetylene ionomers have been investigated in which the importance of internal ion compensation to control various oxidation states have been emphasized.³¹

The average values of the redox couple were calculated for **PPA-Cz-C3**, **PPA-Cz-C6**, and **PPA-Cz-C8** and were found to be 0.461, 0.441, and 0.427 V, respectively. This was calculated from the anodic and cathodic peaks taken as the maximum of both peaks in a precursor polymer-free scan on the substrates after 10 cycles at 50 mV/s in 0.5 mg/mL polymer/CH₂Cl₂ in 0.1 M TBAH. From these data, it can be observed that the redox potential decreased as the length of the alkyl chain increased. Longer alkyl side chains tend to weaken any electron withdrawing effect from the PPA polymer backbone and decrease the redox potential.²⁴ This may also be attributed to a change in the conformation of the polymer backbone influenced by steric effects of the side group. Nevertheless, such property may allow the possibility of band-gap tuning of the HOMO level for these

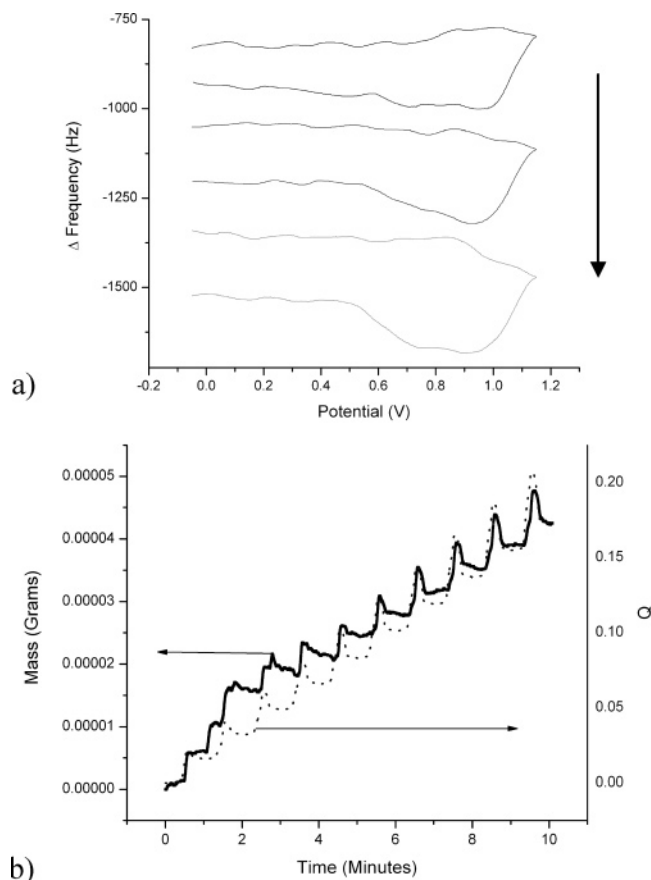


Figure 4. Electrochemical quartz crystal microbalance for **PPA-C6-Cz** at a scan rate of 50mV/s: (a) E-QCM plot of Δ frequency vs potential for cycles 3, 5, and 7. There is a slight increase in the change from the 3rd cycle to the 7th; however the difference in the 6th and 7th cycles and onward is negligible. (b) Mass (g) and amount of charge (Q) vs time plots for E-QCM. After a slight induction period, a fairly linear growth pattern can be seen in both plots.

polymers with respect to device optimization. It should be noted that continuous potential cycling up to 10 cycles below 1.1 V for *all* these polymers, resulted in a linear area increase of the charge per cycle, corresponding to the linear deposition of polymer films. This observation of linear increase is consistent with what we have observed with other precursor polymers and the electropolymerization of PVK.^{18–22} Furthermore, these films are transparent and are insoluble to organic solvents indicating a cross-linked film. For precursor polymers in general, we have observed that a “certain free volume” is necessary for effective cross-linking and film formation.²² In this case, a longer alkyl spacer or decoupling of the electropolymerizable carbazole monomer units results in a more homogeneous film formation.

Electrochemical—Quartz Crystal Microbalance measurements. Electrochemical—quartz crystal microbalance measurements were performed under much the same manner as the corresponding aforementioned CV. The difference from the previous electrochemistry setup is that the working electrode was changed from the Cz modified ITO slide to an unmodified Au coated quartz crystal with a 1.327 cm² working electrode area. The mass deposition per cycle was studied during the electrochemical polymerization (Figure 4). While it is true that viscoelastic effects do play a role in frequency changes when characterizing films by EQCM, it has been shown that EQCM is an effective tool for characterizing sufficiently thin films.³² For thin films (where the film thickness is much less than the wavelength of the piezoelectrically launched shear waves) a simplified form of the mass frequency relation can be used.

From the well-known Sauerbrey equation, the frequency shift ΔF (Hz) is a function of several parameters in the QCM setup.³³ As can be seen in Figure 4b, the trace of the mass gain corresponds to that of the amount of charge transferred to electrode. This indicates that the deposition is due to the oxidation of the pendant carbazole units starting from about 0.9 V in the anodic scan of the CV cycle. The decrease of mass and amount of charge corresponds to the anion dedoping of supporting electrolyte, which confirms the electroactivity of the deposited film. The ΔF vs potential plot shows a regular increase in mass deposited with each cycle upon the cathodic scan. As the scan number increases, a dedoping of supporting electrolyte can also be seen. The plot of mass gain vs time has an induction period at the beginning of the experiment, but after the second cycle, the growth takes on a linear increase, giving a homogeneous film growth. This may be due to the absence of the carbazole SAM “adhesion” layer utilized with the ITO electrodes. However, this induction behavior is typical of most electropolymerization experiments.³² Likewise, E-QCM measurements of several cycles under precursor polymer-free conditions (see Supporting Information) showed no increase in deposited mass (or frequency shift) following each cycle. This is consistent with the reversible CV oxidation–reduction cycle as shown in Figure 3b. Thus, these polymers are well-behaved in terms of their film deposition properties and ion/mass transport.

Spectroelectrochemistry. To observe the presence of both the cross-linked carbazole and polyacetylene backbone species on the deposited film, spectroelectrochemistry measurements were made. UV–vis absorption spectra were measured in situ together with CV film deposition on **PPA-Cz-C6** in 0.1 M TBAH/CH₂Cl₂ electrolyte (WE, modified ITO; CE, Pt wire; RE, Ag/AgCl) at a scan rate of 20 mV s^{−1}. Potentiostatic measurements were then made on this deposited film to show doping/dedoping dependence with potential.

From the CV method, the peak at 550 nm was tracked and showed a linear increase with increasing CV cycle indicating deposition of the polymer (Figure 5a). After completion of the CV deposition, the two peaks at 400 and 850 nm were monitored during a series of potentiostatic measurements between 0 and 1.1 V (Figure 5b). Both peaks increased with higher potential but disappeared at lower and zero potentials. Therefore, the absorbance spectra in Figure 5b shows the doped (oxidized) and dedoped (reduced) states of the deposited films. Since the UV–vis spectra was monitored from a previously deposited film (no electropolymerization taking place), the peaks at 400 and 850 nm can be assigned to the polaronic band originating from the contribution of poly(carbazole) species and their complex ion couple with the hexafluorophosphate ions. The assignments are polaron bonding level to the π^* conduction band for the 400 nm and bonding level to the antibonding state for the 850 nm.³⁴ With active CV deposition, this is not easily observed. Thus, from Figure 5a, the 550 nm peak can be assigned to the π – π^* transition of the polyacetylene, which increases linearly with film deposition during CV cycling.

From these measurements, the band-gap, ΔE_g , could be calculated and compared between the different electroactive species present on the film. The calculated ΔE_g for the cross-linked polycarbazole species was estimated to be 3.13 eV based on extrapolation of the onset of absorbance in the UV–vis for the polycarbazole peak. The ΔE_g for the cross-linked polyacetylene species was calculated from the onset of reduction and oxidation through CV methods and was found to be 2.45 eV. Some of the references for polyacetylene have given ΔE_g CDV

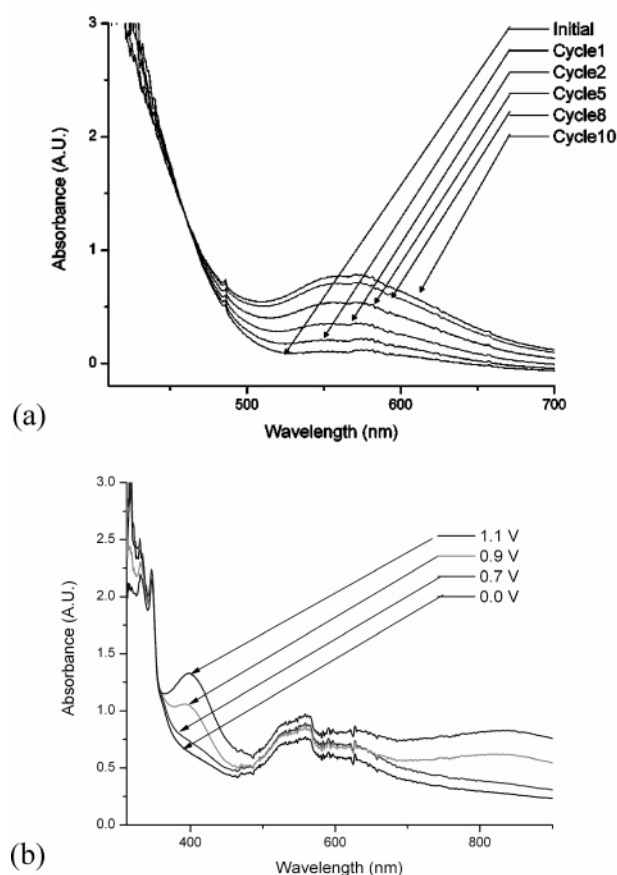


Figure 5. (a) Growth of the 550 nm peak during CV electrodeposition of **PPA-C6-Cz**, spectra taken in situ at 0 V during each CV cycle (b) Doping/dedoping studies with potentiostatic methods on **PPA-C6-Cz**.

values of up to 1.88 eV.³¹ Thus, the results from potentiostatic spectroelectrochemistry methods confirmed the attributes of the PPA double—single bond polymer backbone in the presence of cross-linked polycarbazole units. However, their exact quantitative contribution to the cross-linked structure in the film is not easily distinguished by spectroelectrochemical methods alone.

AFM Imaging. Figure 6 shows the AFM image of the electropolymerized **PPA-C6-Cz** electropolymerized at 80 mV/s in 0.1 M TBAH/CH₂Cl₂ electrolyte (WE, modified ITO; CE, Pt wire; RE, Ag/AgCl wire). Electrochemical polymerization was carried out under CV conditions, for 10 cycles at a range of −50 to +1100 mV at a scan rate of 80 mV s^{−1} on the triethoxy(11-carbazoylundecyl)silane modified ITO plate. The films were optically smooth and uniform both by visual inspection and optical microscopy. The AFM image was made under ambient and dry conditions using MAC mode (noncontact). The morphology consisted of globular features on the order of 100–200 nm diameter which are regular in size and from relatively from large domains. The morphology is similar to that of our previously electrodeposited precursor polymers, e.g., the layer-by-layer electrodeposition of poly(methylhydrosiloxane)-functionalized polythiophenes under CV conditions in which smooth films were formed with each cycle.^{19,32}

Conclusion

This work has shown that carbazole substituted poly(phenylacetylene)s (PPA) can be electrochemically cross-linked and deposited on triethoxy(11-carbazoylundecyl)silane-modified ITO resulting in the formation of conjugated polycarbazole

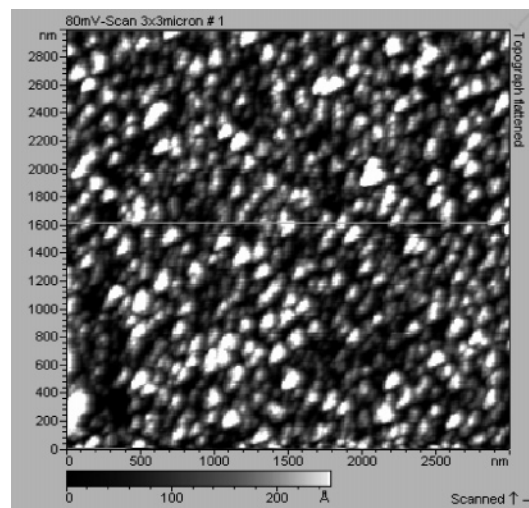


Figure 6. AFM image of the electropolymerized **PPA-C6-Cz** electropolymerized at 80 mV/s in 0.1 M TBAH/CH₂Cl₂ electrolyte on the triethoxy(11-carbazoylundecyl)silane-modified ITO plate (WE, modified ITO; CE, Pt wire; RE, Ag/AgCl wire).

networks without significantly decomposing the backbone. The two redox peaks observed at 0.6 V vs Ag/AgCl and above 1.0 V vs Ag/AgCl as confirmed by CV measurements were due to the carbazole and PPA unit charge complex couples, respectively. Regular and stepwise growth of the films was confirmed through in situ spectroelectrochemistry and electrochemical-QCM. These results emphasize that the following **PPA-PCz-Cn** polymer design is feasible for the electropolymerization of carbazole without affecting the PPA conjugated backbone significantly. The deposition method resulted in a combination of PPA and the PCz properties in one film. This was confirmed on the basis of the electrochemical species being identified (doping and dedoping) and followed using spectroelectrochemical measurements. CV trends with spacer chain length differences and a well-behaved electrochemical deposition and cross-linking behavior should allow HOMO-level and work-function tuning with these materials. Measurements are underway to determine their compatibility in polymer light emitting diode device (PLED) applications as hole transport materials.

Acknowledgment. The authors of this paper would like to express their thanks for the partial funding from the Robert Welch Foundation (E-1551), NSF-DMR (05-04435), NSF-DMR (99-82010), and NSF-CTS (0330127). We would also like to acknowledge technical support from Maxtek Inc. and Molecular Imaging Inc. (now Agilent Technologies).

Supporting Information Available: Figures showing CV scan of PPA control, five cycle CV for electrochemical crosslinking/deposition, and monomer free E-QCM study. This material is available free of charge via the Internet at <http://pubs.acs.org>.

References and Notes

- (1) Work on conjugated and conducting polymers: Heeger, MacDiarmid, and Shirakawa won the Nobel Prize in Chemistry in 2000. Other important references: (a) Shirakawa, H.; Louis, E. J.; MacDiarmid, A. G.; Chiang, C. K.; Heeger, A. J. *J. Chem. Soc., Chem. Commun.* **1977**, 578 (b) Ciardelli, F.; Lanzillo, S.; Pieroni, O. Optically Active Polymers of 1-Alkynes. *Macromolecules* **1974**, *7*, 174–179 (c) Masuda, T.; Higashimura, T. *Acc. Chem. Res.* **1984**, *17*, 51–56.
- (2) (a) Karim, S. M. A.; Nomura, R.; Masuda, T. *J. Polym. Sci., Part A: Polym. Chem.* **2001**, *39*, 3130. (b) Nakako, H.; Nomura, R.; Tabata, M.; Masuda, T. *Macromolecules* **1999**, *32*, 2861.
- (3) Sanda, F.; Kawaguchi, T.; Masuda, T.; Kobayashi, N. *Macromolecules* **2003**, *36*, 2224.

- (4) Sata, T.; Nomura, R.; Wada, T.; Sasabe, H.; Masuda, T. *J. Polym. Sci., Part A: Polym. Chem.* **1998**, *36*, 2489.
- (5) (a) Nagai, K.; Masuda, T.; Nakagawa, T.; Freeman, B. D.; Pinnau, I. *Prog. Polym. Sci.* **2001**, *26*, 721. (b) Masuda, T. Acetylenic Polymers. In *Polymeric Material Encyclopedia*; Salamone, J. C., Ed.; CRC, New York, 1996; Vol. 1, p 32. (c) Hidayat, R.; Fujii, A.; Ozaki, M.; Teraguchi, M.; Masuda, T.; Yoshino, K. *Synth. Met.* **2001**, *119*, 597–598.
- (6) (a) Sun, R.; Masuda, T.; Kobayashi, T. *Synth. Met.* **1997**, *91*, 301–303. (b) Wang, Y.; Sun, R.; Wang, D.; Swager, T. M.; Epstein, A. J. *Appl. Phys. Lett.* **1999**, *74*, 2593–2595 (c) Tang, B. Z.; Xu, H.; Lam, W. Y. *Chem. Mater.* **2000**, *12*, 1446–1455. (d) Xie, Z.; Kwok, H. S.; Tang, B. Z. *Opt. Mater.* **2002**, *21*, 231–234.
- (7) (a) Shiota, Y.; Kakuta, T.; Kanega, H.; Mikawa, H. *J. Chem. Soc., Chem. Commun.* **1985**, 1201. (b) Pearson, J. M.; Stolka, M. *Polymer Monographs*; Gordon and Breach, New York, 1981; Vol. 6.
- (8) Burrows, P. E.; Forrest, S. R.; Sibley, S. P.; Thompson, M. E. *Appl. Phys. Lett.* **1996**, *69*, 2959.
- (9) Mori, T.; Obata, K.; Inaizumi, K.; Mizutani, T. *Appl. Phys. Lett.* **1996**, *69*, 3309.
- (10) Michelotti, F.; Borghese, F.; Bertolotti, M.; Cianci, E.; Foglietti, V. *Synth. Met.* **2000**, *111*, 105.
- (11) Tamada, M.; Omichi, H.; Okui, N. *Thin Solid Films* **1995**, *268*, 18.
- (12) Papez, V.; Josowicz, M. *J. Electroanal. Chem.* **1994**, *365*, 139.
- (13) Kido, J.; Shionoya, H.; Nagai, K. *Appl. Phys. Lett.* **1995**, *67*, 2281.
- (14) (a) Kawde, R.; Santhanam, K. *Bioelectrochem. Bioeng.* **1995**, *38*, 405. (b) Laxmeshwar, N.; Kawde, R.; Santhanam, K. *Sens. Actuators* **1995**, *23*, 35.
- (15) (a) Skompska, M.; Hillman, A. R. *J. Electroanal. Chem.* **1997**, *433*, 127. (b) Borjas, R.; Buttry, D. A. *J. Electroanal. Chem.* **1990**, *280*, 73.
- (16) (a) Romero, D.; Nuesch, F.; Benazzi, T.; Ades, D.; Siove, A.; Zuppiroli, L. *Adv. Mater.* **1997**, *9*, 1158. (b) Ambrose, J.; Carpenter, L.; Nelson, R. *J. Electrochem. Soc.* **1975**, *122*, 876.
- (17) (a) Desbene-Monvernay, A.; Dubois, J. E.; Lacaze, P. C. *J. Electroanal. Chem.* **1985**, *189*, 51. (b) Papez, V.; Inganas, O.; Cimrova, V.; Nespurek, S. *J. Electroanal. Chem.* **1990**, *282*, 123. (c) Skompska, M.; Peter, L. M. *J. Electroanal. Chem.* **1995**, *383*, 43.
- (18) (a) Sebastian, R.; Caminade, A.; Majoral, J.; Levillain, E.; Huchet, L.; Roncali, J. *Chem. Commun.* **2000**, *6*, 507 (b) Deng, S.; Advincula, R. *Chem. Mater.* **2002**, *14*, 4073. (c) Taranekekar, P.; Fan, X.; Advincula, R. *Langmuir* **2002**, *18*, 7943. (d) Inaoka, S.; Advincula, R. *Macromolecules* **2002**, *35*, 2426. (e) Park, M.-K.; Xia, C.; Advincula, R. C.; Schutz, P.; Caruso, F. *Langmuir* **2001**, *17*, 7670. (f) Watson, K.; Wolfe, P.; Nguyen, S.; Zhu, J.; Mirkin, C. *Macromolecules* **2000**, *33*, 4628. (g) Jang, S.-Y.; Sotzing, G. A.; Marquez, M. *Macromolecules* **2002**, *35*, 7293.
- (19) Xia, C.; Fan, X.; Park, M.; Advincula, R. *Langmuir* **2001**, *17*, 7893.
- (20) Onishi, K.; Advincula, R. C.; Karim, S. M. A.; Nakai, T.; Masuda, T. *Polym. Prepr. (Am. Chem. Soc., Div. Polym. Chem.)* **2002**, *43* (1), 171.
- (21) (a) Baba, A.; Onishi, K.; Knoll, W.; Advincula, R. C. *J. Phys. Chem. B* **2004**, *108*, 18949. (b) Xia, C.; Advincula, R. C.; Baba, A.; Knoll, W.; *Chem. Mater.* **2004**, *16*, 2852–2856. (c) Inaoka, S.; Roitman, D.; Advincula, R. In *Forefront of Lithographic Materials Research*; Ito, H., Khojasteh, M., Li, W., Eds. Kluwer Academic Publishers: New York, 2001; p 239. (d) Xia, C.; Inaoka, S.; Roitman, D.; Advincula, R. In *Thin Films: Preparation, Characterization, Applications*; Soriaga, M., Stickney, J., Bottomley, L., Eds.; Plenum Publishers: New York, 2002; p. 197.
- (22) Xia, C.; Advincula, R. *Chem. Mater.* **2001**, *13*, 1682.
- (23) Sanda, F.; Nakai, T.; Kobayashi, N.; Masuda, T. *Macromolecules* **2004**, *37*, 2703.
- (24) (a) Persigehl, P.; Jordan, R.; Nuyken, O. *Macromolecules* **2000**, *33*, 6977. (b) Barrett, C.; Choudhury, B.; Natasohn, A.; Rochon, P. *Macromolecules* **1998**, *31*, 4845. (c) Sonogashira, K.; Tohda, H.; Hagihara, N. *Tetrahedron Lett.* **1975**, 4467.
- (25) Masuda, T.; Takahashi, T.; Yamamoto, K.; Higashimura, T. *J. Polym. Sci Part A: Polym. Chem.* **1982**, *20*, 2603.
- (26) Han, B. H.; Boudjouk, P. *Organometallics* **1983**, *2*, 769.
- (27) Nakano, M.; Masuda, T.; Higashimura, T. *Polym. Bull. (Berlin)* **1995**, *34*, 191.
- (28) Garcia-Canadas, J.; Lafuente, A.; Rodriguez, G.; Marcos, M.; Velasco, J. *J. Electroanal. Chem.* **2004**, *565*, 57. (b) Baker, C.; Reynolds, J. R. *J. Electroanal. Chem.* **1987**, *251*, 307–322. (c) Baba, A.; Tian, S.; Stefani, F.; Xia, C.; Wang, Z.; Advincula, R.; Johannsmann, D.; Knoll, W. *J. Electroanal. Chem.* **2004**, *562*, 95–103. (d) Baba, A.; Kaneko, F.; Advincula, R. C. *Colloids Surf. A* **2000**, *173*, 39–49. Garcia-Canadas, J.; Lafuente, A.; Rodriguez, G.; Marcos, M.; Velasco, J. *J. Electroanal. Chem.* **2004**, *565*, 57.
- (29) (a) Baba, A.; Onishi, K.; Knoll, W.; Advincula, R. C. *J. Phys. Chem. B* **2004**, *108*, 18949. (b) Hilger, A.; Gisselbrecht, J. P.; Tykwinski, R.; Boudon, C.; Schrieber, M.; Martin, R.; Lüthi, H.; Gross, M.; Diederich, F. *J. Am. Chem. Soc.* **1997**, *119*, 2069.
- (30) Jozefiak, T. H.; Ginsburg, E. J.; Gorman, C. B.; Grubbs, R. H.; Lewis, N. S. *J. Am. Chem. Soc.* **1993**, *115*, 4705.
- (31) Loneragan, M. C.; Cheng, C. H.; Langsdorf, B. L.; Zhou, X. *J. Am. Chem. Soc.* **2002**, *124*, 690.
- (32) Taranekekar, P.; Baba, A.; Fulghum, T. M.; Advincula, R. *Macromolecules* **2005**, *38*, 3679.
- (33) Sauerbrey, G. *Z. Phys.* **1959**, *155*, 206.
- (34) Sezer, E.; Ustamehmotoglu, A.; Sarac, S. *Synth. Met.* **1999**, *107*, 7.

MA0510946